


RESEARCH PAPER

Critical role of OX40 in drug-induced acute liver injury

Chunpan Zhang^{1,5} | Hua Jin^{1,2,3,4} | Yan Wang⁵ | Changying Li^{1,2,3,4} |
 Xinyan Zhao⁵ | Yanmeng Li² | Wen Shi^{1,2,3,4} | Yue Tian^{1,2,3,4} |
 Hufeng Xu^{1,2,3,4} | Dan Tian^{1,2,3,4} | Kai Liu^{1,2,3,4} | Jidong Jia^{5,6} |
 Guangyong Sun^{1,2,3,4} | Dong Zhang^{1,2,3,4,6,7} 

¹General Surgery Department, Beijing Friendship Hospital, Capital Medical University, Beijing, China

²Experimental and Translational Research Center, Beijing Friendship Hospital, Capital Medical University, Beijing, China

³Immunology Research Center, Beijing Clinical Research Institute, Beijing, China

⁴Beijing Key Laboratory of Tolerance Induction and Organ Protection in Transplantation, Beijing Friendship Hospital, Beijing, China

⁵Liver Research Center, Beijing Friendship Hospital, Capital Medical University, Beijing, China

⁶National Clinical Research Center for Digestive Diseases, Beijing Friendship Hospital, Beijing, China

⁷Immunology Research Center for Oral and Systemic Health, Beijing Friendship Hospital, Capital Medical University, Beijing, China

Correspondence

Jidong Jia, Liver Research Center, Beijing Friendship Hospital, Capital Medical University, Beijing 100050, China.
 Email: jia_jd@ccmu.edu.cn

Guangyong Sun and Dong Zhang, General Surgery Department, Beijing Friendship Hospital, Capital Medical University, Beijing 100050, China.
 Email: sunguangyonga@163.com; zhangd@ccmu.edu.cn

Funding information

National Natural Science Foundation of China, Grant/Award Numbers: 81870399, 81900526, 81970503

Background and Purpose: The innate and adaptive immune systems both play important roles in drug-induced liver injury (DILI). However, the crosstalk between the innate and adaptive immunity in DILI is largely unknown. Extensive crosstalk is likely mandated by co-stimulatory interactions between these immune systems. OX40 is a co-stimulatory molecule, but whether it regulates the intrahepatic immune response in DILI remains unknown.

Experimental Approach: Acute liver injury was induced by paracetamol (acetaminophen), carbon tetrachloride (CCl₄), and D-galactosamine/LPS (GalN/LPS) in wild-type (WT) and OX40 knockout (KO) mice, and disease progress was compared.

Key Results: Plasma OX40 levels were significantly increased and were augmented in intrahepatic CD4⁺ T cells after paracetamol, CCl₄, or GalN/LPS administration. Liver injury in OX40-deficient mice was attenuated compared with that in WT mice. Compared with WT mice, hepatic infiltration of Th1 and Th17 cells and macrophages in OX40 KO mice was reduced. Furthermore, adoptive transfer of OX40 KO-CD4⁺ T cells to Rag1^{-/-} mice resulted in alleviated liver injury compared with WT-CD4⁺ T-cell transfer, with reduced liver infiltration of macrophages and pro-inflammatory cytokine secretion. Moreover, OX40/Fc stimulation in vitro revealed that soluble OX40 enhanced the biological function of murine macrophages, including up-regulation of genes associated with inflammation and tissue infiltration. Finally, soluble OX40 levels were significantly elevated in DILI patients compared with healthy controls.

Conclusion and Implications: OX40 is a key molecule that promotes both pro-inflammatory macrophage and CD4⁺ T-cell function, exacerbating paracetamol-induced liver injury. OX40 could serve as a diagnostic index and therapeutic target of DILI.

Abbreviations: ALB, albumin; ALI, acute liver injury; ALT, alanine aminotransferase; APAP, acetaminophen or paracetamol; APC, antigen-presenting cell; AST, aspartate aminotransferase; CCl₄, carbon tetrachloride; CYP2E1, hepatic cytochrome P4502E1; DBIL, direct bilirubin; DILI, drug-induced liver injury; GalN, D-galactosamine; Hif1 α , hypoxia-inducible factor 1 alpha; MNC, mononuclear cell; NAPQI, N-acetyl-p-benzoquinone imine; RT-PCR, reverse transcription-polymerase chain reaction; TBIL, total bilirubin.

Chunpan Zhang, Hua Jin, and Yan Wang contributed equally to this study.

1 | INTRODUCTION

Drug-induced liver injury (DILI) is a term used to describe unexpected damage to the liver, including hepatocyte and other liver cell damage, caused by commonly used drugs (Andrade et al., 2019). **Paracetamol**, also known as acetaminophen (APAP), is a widely used analgesic and antipyretic drug. However, paracetamol overdose causes acute liver injury (ALI) or acute liver failure (Jaeschke, Williams, Ramachandran, & Bajt, 2012). Paracetamol is metabolized to **N-acetyl-p-benzoquinone imine** (NAPQI) by **cytochrome P4502E1** in the hepatocyte, over-accumulation of which could damage the mitochondrial function via **GSH** consumption that accompanies oxidative stress. Furthermore, damaged hepatocyte releases danger-associated molecular patterns, including high-mobility group box 1, **heat shock protein 70** and DNA fragments. These danger-associated molecular patterns activate innate immune cells, for example, antigen-presenting cells (APCs), which release various inflammasomes (Kim et al., 2017; Mossanen & Tacke, 2015).

Innate immune cells are activated and believed to play critical roles in paracetamol-induced liver injury (Jaeschke et al., 2012; Krenkel, Mossanen, & Tacke, 2014). According to recent studies, innate immunity and adaptive immunity both play important roles in paracetamol-induced liver injury. T cells aggravate paracetamol hepatotoxicity by producing **IFN- γ** and **TNF- α** and increasing **STAT1** activation, while decreasing **STAT3** activation in the hepatocyte (Numata et al., 2007). In addition, Th1 cells, but not CD8⁺ T cells, exacerbate acute liver injury via IFN- γ and **IL-2**, while Treg cells alleviate liver injury depending on the secretion of **IL-10** and **TGF- β** (Wang et al., 2015). Further, the numbers of Th17 cells producing **IL-17A** rapidly increase in the liver in response to paracetamol-induced liver injury (Zhu & Uetrecht, 2013).

As one of the co-stimulatory molecules, **OX40** is mainly expressed on activated, memory and regulatory CD4⁺ T cells and to a lesser degree on CD8⁺ T cells, but not on naïve cells (Croft, So, Duan, & Soroosh, 2009). OX40 is activated by its cognate ligand **OX40L**, found on antigen-presenting cells. In naïve CD4⁺ T cells, OX40 engagement can lead to either Th1 or Th2 cell generation in different disease models, depending on the micro-environment (Croft et al., 2009; Ward-Kavanagh, Lin, Sedy, & Ware, 2016). However, whether OX40 can regulate the intrahepatic immune response in paracetamol-induced acute liver injury remains unknown. Therefore, in the current study, we explored the role of OX40 in paracetamol-induced hepatotoxicity and examined the function of OX40 in regulating the interaction of intrahepatic innate and adaptive immunity.

2 | METHODS

2.1 | Mice

Eight-week-old male C57BL/6 wild-type (WT), C57BL/6-Ox40-KO (Ox40 KO), and B6.Rag1 KO (*Rag1*^{-/-}) mice (average weight 20–25 g) were purchased from Beijing Vital River Laboratory (Beijing, China).

What is already known

- The innate and adaptive immune systems both play important roles in drug-induced liver injury (DILI).
- OX40 promotes T-cell activation, survival and cytokine production.

What this study adds

- OX40 levels and OX40 expression by intrahepatic CD4⁺T cells are significantly elevated during DILI.
- OX40 enhances pro-inflammatory macrophage polarization during DILI by increasing Hif1 α expression.

What is the clinical significance

- OX40 may serve as a diagnostic index and therapeutic target of DILI.

The mice were housed in a specific pathogen-free, temperature-controlled environment, with free access to food and water at the animal facilities at Beijing Friendship Hospital (Beijing, China). All experimental procedures were conducted in accordance with the protocol approved by the Institutional Animal Care and Ethics Committee at Beijing Friendship Hospital (approval number IACUC ID: 18-2009). The study was designed to generate groups of equal size, using randomization and blinded analysis. Animal studies are reported in compliance with the ARRIVE guidelines (Kilkenny, Browne, Cuthill, Emerson, & Altman, 2010) and with the recommendations made by the *British Journal of Pharmacology* (McGrath, Drummond, McLachlan, Kilkenny, & Wainwright, 2010; McGrath & Lilley, 2015).

2.2 | Induction of acute liver injury

Paracetamol (Sigma-Aldrich, St. Louis, MO, USA) was dissolved in phosphate buffer solution (PBS) by warming at 40°C. WT and Ox40 KO mice were randomly administered PBS ($n = 5$) or paracetamol ($n = 6$; 150, 200, 250 or 300 mg·kg⁻¹) via i.p. injection after fasting for 12 hr. *Rag1*^{-/-} mice were randomly divided into PBS and paracetamol-induced acute liver injury groups ($n = 5$) and treated as WT and Ox40 KO mice. The mice were killed 24 hr after paracetamol injection.

For the carbon tetrachloride (CCl₄)-induced mouse model of acute liver injury, WT and Ox40 KO mice were fasted for 12 hr and randomly divided into treatment and control groups. The treatment group animals ($n = 6$) were i.p. injected 10 ml·kg⁻¹ body weight of a mixed solution of CCl₄ (Sinopharm, Shanghai, China) and olive oil (Sigma; 1:7 volume ratio). The control group animals ($n = 5$) were i.p. injected an equal volume of olive oil. The animals were killed 24 hr after CCl₄ injection.

For the mouse model of D-galactosamine (GalN) and LPS-induced acute liver injury, after fasting for 12 hr, WT and Ox40 KO mice were randomly divided into treatment and control groups. The treatment group animals ($n = 6$) were i.p. injected $220 \text{ mg}\cdot\text{kg}^{-1}$ of D-galactosamine (Sigma) and $5 \mu\text{g}\cdot\text{kg}^{-1}$ of LPS (Sigma). The control group animals ($n = 5$) were i.p. injected an equal volume of PBS. The mice were killed 8 hr after GalN/LPS administration, and liver injury and intrahepatic immune response were evaluated, as described below.

2.3 | Antibodies and reagents

Fluorochrome-conjugated antibodies against mouse NK1.1 (clone PK136, Cat#: 12-5941-83, RRID:AB_466051), CD3 (clone 145-2C11, Cat#: 17-0031-83, RRID:AB_469316), CD4 (clone GK1.5, Cat#: 11-0041-85, RRID:AB_464893), CD8 (clone 53-6.7, Cat#: 45-0081-82, RRID:AB_1107004), CD45 (clone 30-F11, Cat#: 25-0451-82, RRID:AB_469625), CD45.1 (clone A20, Cat#: 25-0453-82, RRID:AB_469629), CD11b (clone M1/70, RRID:AB_465549, RRID:AB_465549), Ly6G (clone 1A8-Ly6g, Cat#: 17-9668-82, RRID:AB_2573307), F4/80 (clone BM8, Cat#: 17-4801-82, RRID:AB_2784648), OX40L (clone OX86, Cat#: 17-1341-82, RRID:AB_10717260), TNF- α (MP6-XT22, Cat#: 12-7321-82, RRID:AB_466199), OX40 (clone OX-86, Cat#: 17-1341-82, RRID:AB_10717260), IFN- γ (clone XMG1.2, Cat#: 12-7311-82, RRID:AB_466193), IL-17A (clone eBio17B7, Cat#: 12-7177-81, RRID:AB_763582), IL-6 (clone MQ2-13A5, Cat#: 12-7061-82, RRID:AB_466168) and IL-10 (clone JES5-16E3, Cat#: 12-7101-82, RRID:AB_466176) were obtained from Thermo Fisher Scientific (Inc., Pittsburgh, PA, USA). Anti-PE microbeads were purchased from Miltenyi Biotec (Auburn, CA, USA).

2.4 | Plasma levels and intrahepatic mononuclear cell assays

Alanine aminotransferase (ALT) and aspartate aminotransferase (AST) plasma levels were determined by using the appropriate kits purchased from the Nanjing Jiancheng Biochemical Institute (Nanjing, Jiangsu, China), following the manufacturer's instructions. Soluble OX40 plasma levels were determined by using an ELISA kit (Boster Biological Technology, Hubei, China), as recommended by the manufacturer.

The liver tissue was digested using 0.01% collagenase IV (Sigma-Aldrich) and the intrahepatic mononuclear cells (MNCs) were isolated and purified by 30%/70% Percoll (GE Healthcare, Uppsala, Sweden) density gradient centrifugation, as previously described (Mederacke, Dapito, Affo, Uchinami, & Schwabe, 2015).

2.5 | CD4⁺ T isolation and adoptive transfer

The splenocytes were isolated from WT and Ox40 KO mice. The red blood cells were subsequently removed by using erythrocyte lysis

buffer (Qiagen, Valencia, CA, USA). CD4⁺ T cells (purity >95%) were obtained by FACS (BD Biosciences, San Diego, CA, USA). Approximately 5×10^6 purified WT-CD4⁺ T cells or Ox40 KO-CD4⁺ T cells were transferred into naïve *Rag1*^{-/-} mice by tail vein injection ($n = 5$). Control group was injected an equal volume of PBS via tail vein ($n = 5$). Then these mice were fasted for 12 hr and followed by administration of paracetamol ($300 \text{ mg}\cdot\text{kg}^{-1}$). The mice were killed 24 hr after the paracetamol challenge.

2.6 | Soluble OX40 stimulation in vivo

Rag1^{-/-} mice were i.p. injected with $3 \mu\text{g}$ of OX40/Fc ($n = 5$; R&D Systems, Minneapolis, MN, USA) or control IgG ($n = 5$). The mice were then fasted for 12 hr, and $300 \text{ mg}\cdot\text{kg}^{-1}$ paracetamol or $150 \text{ mg}\cdot\text{kg}^{-1}$ paracetamol were i.p. injected. The mice were killed 24 hr after the paracetamol challenge.

2.7 | Cell culture

RAW264.7 and J774A.1 cells were purchased from China Infrastructure of Cell Line Resource. The macrophage cell lines were routinely grown in a culture vessel in Dulbecco's modified Eagle medium with L-glutamine supplemented with 10% fetal bovine serum, penicillin, and streptomycin. The cultures were maintained at 37°C, under a humidified atmosphere of 5% CO₂. The cells were cultured with OX40/Fc (0.5, 1.0, or 2.0 $\mu\text{g}\cdot\text{ml}^{-1}$) or the IgG control (2.0 $\mu\text{g}\cdot\text{ml}^{-1}$) for 48 hr before harvesting. To block the activity of OX40/Fc, the macrophage lines were pretreated with OX40L (0.5 $\mu\text{g}\cdot\text{ml}^{-1}$, R&D Systems) for 6 hr.

2.8 | Determination of plasma cytokine levels

Cytokine levels in the mouse plasma were examined using LEGENDplex™ mouse inflammation panel (Biolegend, CA, USA), according to the manufacturer's instructions.

2.9 | Determination of GSH levels in liver tissue

The extent of oxidative stress was determined in liver homogenates by measuring GSH levels using commercial kits (Nanjing Jiancheng) according to the manufacturer's protocol.

2.10 | Western blotting

Liver tissue (20 mg) was solubilized in RIPA (Solarbio, Beijing, China) on ice for 20 min. The protein concentration was then determined using BCA protein assay, as recommended by the manufacturer. Protein mixtures was normalized to 40 μg and loaded into each well and

separated by 10% SDS-PAGE. Following a 2-hr run, the proteins were electrophoretically transferred onto PVDF membrane. The membranes were blocked in 5% non-fat dry milk and subsequently incubated with a rabbit polyclonal antibody against hepatic cytochrome P4502E1 (CYP2E1; Abcam, Cat# ab28146; 1:5,000 dilution) and mouse monoclonal antibody against GAPDH (Abcam, Cat# EPR16891; 1:1,000 dilution) at 4°C overnight. The immuno-related procedures used comply with the recommendations made by the *British Journal of Pharmacology* (Alexander et al., 2018).

2.11 | Reverse-transcription PCR

Total RNA was extracted from the liver tissue, intrahepatic mononuclear cells, and RAW264.7 and J774A.1 cells using an RNeasy Plus Mini Kit (Qiagen) in accordance with the manufacturer's protocol and reverse-transcribed to cDNA using a SuperScript III RT kit (Invitrogen, Carlsbad, VA, USA). Quantitative real-time PCR analysis was performed using an ABI 7500 Sequence Detection System (Applied Biosystems, Foster City, CA, USA). The PCR mixture consisted of 10 µl of SYBR Green Master Mix, 0.5 µM of the forward and reverse primers and 1 µl of cDNA sample. Gene expression was normalized to that of *Gapdh*; after normalization, the gene expression was quantified using the $2^{-\Delta\Delta C_t}$ method. The genes and primer sequences are listed in Table S1.

2.12 | Flow cytometry analysis

Cells from mice or culture were harvested, and the expression of various cell surface markers was analysed. To analyse cytokine production by intracellular staining, the cells were fixed and permeabilised using IC fixation buffer and permeabilization buffer (eBioscience), respectively, according to the manufacturer's instruction. All samples were analysed using an Aria II flow cytometer (BD Biosciences), and the data were analysed using FlowJo software v10 (Treestar, Ashland, OR, USA).

2.13 | Clinical study

The diagnosis of drug-induced liver injury is based on the clinical assessment, the knowledge of potential causative drugs of liver injury and the pathological phenotype of liver biopsy (Cavalieri & D'Agostino, 2017; European Association for the Study of the Liver. Electronic address: easloffice@easloffice.eu et al., 2019). Patients with diabetes, non-alcoholic steatohepatitis, alcoholic fatty liver, autoimmune hepatitis and viral hepatitis were excluded. Twenty-six drug-induced liver injury patients with pathological manifestations of drug-induced liver injury underwent a liver biopsy. Of these, 23 patients had a history of taking herbal and/or dietary supplements prior to the onset of liver injury. One patient had taken statins and two patients had taken non-steroidal anti-inflammatory drugs. Thirty-one patients visiting the Physical Examination Center at Beijing Friendship Hospital for routine physical examinations served as healthy controls. Healthy

subjects were non-diabetic and without major organ disease, chronic inflammatory conditions, cancer, active psychiatric disease and surgical history. Plasma OX40 levels were determined before treatment. All subjects provided written informed consent before participating in the study, and the study protocol was approved by the Human Institutional Review Board of Beijing Friendship Hospital.

2.14 | Data and analysis

The data and statistical analysis comply with the recommendations of the *British Journal of Pharmacology* on experimental design and analysis in pharmacology (Curtis et al., 2018). Independent values were analysed. Statistical analysis was only undertaken for groups with sizes of a minimum of $n = 5$ independent values. To control for unwanted sources of variation, data were normalized. In this current study, the results of reverse-transcription PCR (RT-PCR) and CYP2E1 determined by western blot, as well as the mean fluorescence intensity analysis, were normalized to matched controls for comparison and quantification (the matched control value was set as 100%). Outliers were included in data analysis and presentation. All analyses were done using SAS version 9.3 (SAS Inc., Cary, NC, USA) and Prism 6.0 software (GraphPad Software, San Diego, CA, USA). The values are expressed as the mean \pm SEM. Normal distributions were tested using Shapiro–Wilk test. Differences between groups were evaluated using chi-square test for categorical variables, unpaired Student's *t*-test/one-way ANOVA analysis for normally distributed variables and the Mann–Whitney *U* test for non-normally distributed continuous variables. Post hoc Bonferroni tests were performed for multiple comparisons only if *F* achieved $P < .05$ in ANOVA analysis and there was no significant variance inhomogeneity. Spearman's correlation coefficient was used to estimate the association of plasma OX40 levels and several factors of interest. For all analyses, values of $P < .05$ were considered to be statistically significant.

2.15 | Nomenclature of targets and ligands

Key protein targets and ligands in this article are hyperlinked to corresponding entries in <http://www.guidetopharmacology.org>, the common portal for data from the IUPHAR/BPS Guide to PHARMACOLOGY (Harding et al., 2018), and are permanently archived in the Concise Guide to PHARMACOLOGY 2019/20 (Alexander et al., 2019a,b).

3 | RESULTS

3.1 | Ox40 deficiency attenuates drug-induced liver injury

As shown in Figure 1a, the plasma alanine aminotransferase and aspartate aminotransferase levels increased with the increasing dose

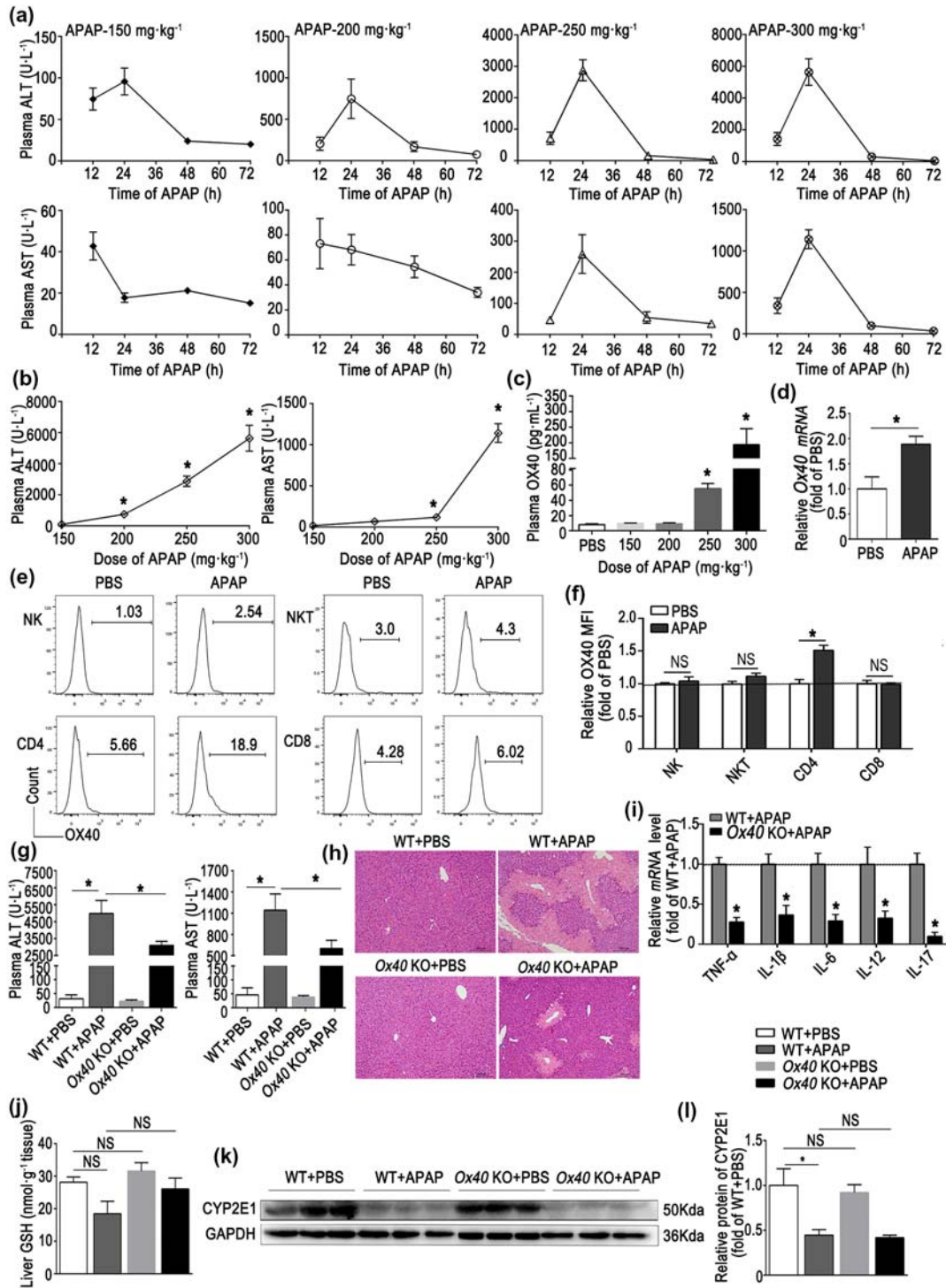


FIGURE 1 Ox40 deficiency attenuates liver injury after paracetamol (APAP) overdose. Acute liver injury (ALI) was induced in C57BL/6 WT by i.p. injecting 150, 200, 250 or 300 mg·kg⁻¹ paracetamol. The control animals were injected the same volume of PBS. (a) Alanine aminotransferase (ALT) and aspartate aminotransferase (AST) plasma levels 12, 24, 48 and 72 hr after paracetamol injection. (b) ALT and AST plasma levels 24 hr after APAP challenge. (c) Soluble OX40 levels were determined by ELISA in PBS and APAP with four doses. (d) *Ox40* mRNA level in hepatic mononuclear cell (MNCs) from the PBS group and 300 mg·kg⁻¹ APAP group. (e) Representative flow cytometry images of OX40⁺ cells among intrahepatic NK, NKT, CD4⁺ and CD8⁺ T cells. (f) Statistical analysis of OX40 levels in intrahepatic NK, NKT, CD4⁺ and CD8⁺ T cells, as determined by flow cytometry. (g) ALT and AST plasma levels at 24 hr after injection of 300 mg·kg⁻¹ APAP. (h) Liver histology (H&E staining) 24 hr after administration of 300 mg·kg⁻¹ APAP. Centrilobular necrosis, bridging necrosis, and massive hepatocyte death are apparent. Original magnification, 100x; scale bar, 200 μm. (i) Relative levels of pro-inflammatory cytokine mRNA in liver tissue, analysed by quantitative real-time PCR. (j) Hepatic GSH levels. (k.) Western blot analysis of CYP2E1 in liver tissue. The data are presented as the mean ± SEM; control groups (n = 5) and treatment groups (n = 6). Two-group comparisons were made by the Student's *t* test, and multiple comparisons were analysed by one-way ANOVA followed by Bonferroni's post hoc test. **P* < .05. NS, no significance

of paracetamol, with the highest alanine aminotransferase and aspartate aminotransferase levels 24 hr after paracetamol administration. The highest alanine aminotransferase and aspartate aminotransferase levels were observed in mice administered 300 mg·kg⁻¹ paracetamol, 24 hr after administration (Figure 1b). Further, the soluble OX40 levels also increased in a dose-dependent manner (Figure 1c). As shown in Figure 1d, compared with PBS-treated controls, OX40 mRNA levels in intrahepatic mononuclear cells were remarkably enhanced in mice treated with paracetamol. Furthermore, OX40 expression was significantly elevated on CD4⁺ T cells after paracetamol administration but not on CD8⁺ T, NK (CD3⁺NK1.1⁺) and NKT (CD3⁺NK1.1⁺) cells (Figure 1e,f). The gating strategy for intrahepatic lymphocytes is shown in Figure S1.

To examine the potential role of OX40 in paracetamol hepatotoxicity, we challenged WT and OX40 KO mice with 300 mg·kg⁻¹ paracetamol. As shown in Figure 1g, the alanine aminotransferase and aspartate aminotransferase levels 24 hr after paracetamol administration were significantly reduced in OX40 KO mice relative to the WT. Histopathological examination indicated a substantially more pronounced centrilobular necrosis and bridging necrosis and massive hepatocyte death in WT mice, with a relatively reduced hepatocyte necrosis in OX40 KO mice during acute liver injury (Figure 1h). As shown in Figure 1i, compared with the WT mice treated with paracetamol for 24 hr, mRNA levels of several cytokines, such as TNF- α , IL-1 β , IL-6, IL-12 and IL-17, were markedly decreased in the liver of OX40 KO mice. We made similar observations for acute liver injury induced by CCl₄ and GalN/LPS (Figures S2 and S3).

Paracetamol is metabolized to *N*-acetyl-*p*-benzoquinone imine by cytochrome P450. In the hepatocyte, CYP2E1 is the key enzyme involved in the process (Zhao et al., 2019). Therefore, we next determined the CYP2E1 and GSH levels during liver injury in WT mice and OX40 KO mice. As shown in Figure 1j-l, no difference in liver GSH and CYP2E1 levels between WT and OX40 KO mice was apparent in the absence of paracetamol challenge. Although slightly decreased, there was no significant reduction in GSH levels at 24 hr after paracetamol injection. However, the hepatic CYP2E1 levels were significantly reduced after paracetamol administration in both WT and OX40 KO mice, but with no difference between the WT and OX40 KO mice after the paracetamol challenge. These observations indicated that OX40 KO regulated the immune response in the damaged liver and alleviated drug-induced acute liver injury.

3.2 | OX40 regulates Th1 and Th17 cell differentiation in drug-induced liver injury

To determine the role of OX40 in paracetamol-induced liver injury, we next examined the immune response in the liver of paracetamol-treated mice. As shown in Figure 2a,b, the percentage of apoptotic CD4⁺ T cells was reduced during acute liver injury. Compared with WT mice, OX40 KO promoted CD4⁺ T-cell apoptosis, but not CD8⁺ T-cell apoptosis in acute liver injury. Meanwhile, the proportions of CD4⁺ and CD8⁺ T cells that were also CD69⁺ dramatically increased

in the liver of WT mice treated with paracetamol compared with the PBS-treated controls (Figure 2c). However, upon paracetamol administration, the hepatic CD4⁺CD69⁺ T-cell percentage, but not CD8⁺CD69⁺ T-cell percentage, was significantly decreased in OX40 KO mice. These observations indicated that OX40 KO promoted apoptosis and reduced activation of CD4⁺ T cells in the paracetamol-treated mice.

Furthermore, we examined the cytokine secretion by hepatic CD4⁺ T cells after paracetamol treatment. As shown in Figure 2d,e, IFN- γ and IL-17A production by CD4⁺ T cells was significantly reduced in the OX40 KO mice relative to the WT mice.

Although Tregs play critical roles in paracetamol-induced acute liver injury (Wang et al., 2015) and OX40 is important for Treg proliferation, in the current study, no significant difference in the proportion of liver-infiltrating CD4⁺Foxp3⁺ T cells was apparent between the OX40 KO and WT mice after paracetamol treatment. In accordance with the analysis of the liver tissue, the IFN- γ and IL-17A plasma levels were also reduced during paracetamol-induced acute liver injury in OX40 KO mice (Figure 2f). These observations demonstrated that OX40 deficiency mainly inhibited CD4⁺ T-cell Th1 and Th17 differentiation in paracetamol-induced acute liver injury.

We observed similar effects (i.e. OX40 KO promoted CD4⁺ T-cell apoptosis and inhibited of Th1 and Th17 cell differentiation) in CCl₄ and GalN/LPS-induced acute liver injury models (Figures S2 and S3).

3.3 | OX40 deficiency down-regulates hepatic macrophage proportion, migration and TNF- α secretion

We observed that the number of monocyte-derived macrophages (CD11b^{int}F4/80^{low}) infiltrating the damaged liver sharply increased after the paracetamol challenge. Furthermore, compared with the WT mice treated with paracetamol, the numbers of intrahepatic-infiltrating macrophages markedly decreased in the OX40 KO mice (Figure 3a). Furthermore, the percentage of Kupffer cells (CD11b^{low}F4/80^{hi}) in the liver of WT mice was reduced after paracetamol treatment. However, there was no significant difference in the percentage of Kupffer cells in the WT and OX40 KO mice.

As shown in Figure 3b,c, the OX40L and CCR5 levels were remarkably elevated in hepatic macrophages in the paracetamol-treated WT mice. However, upon paracetamol administration, the expression of OX40L and CCR5 on intrahepatic macrophages was clearly reduced in OX40 KO mice. No significant difference in the OX40L and CCR5 expression on Kupffer cells between the WT and OX40 KO mice were apparent.

The TNF- α and IL-6 levels were both dramatically increased in macrophages and Kupffer cells in the liver of the paracetamol-treated WT mice (Figure 3d-f). The proportion of TNF- α - and IL-6-positive macrophages, but not that of TNF- α - or IL-6-positive Kupffer cells, in OX40 KO mice was lower than that in the WT mice. However, neither the proportion of IL-10-positive macrophages nor the percentage of IL-10-positive Kupffer cells, as anti-inflammatory cells, significantly

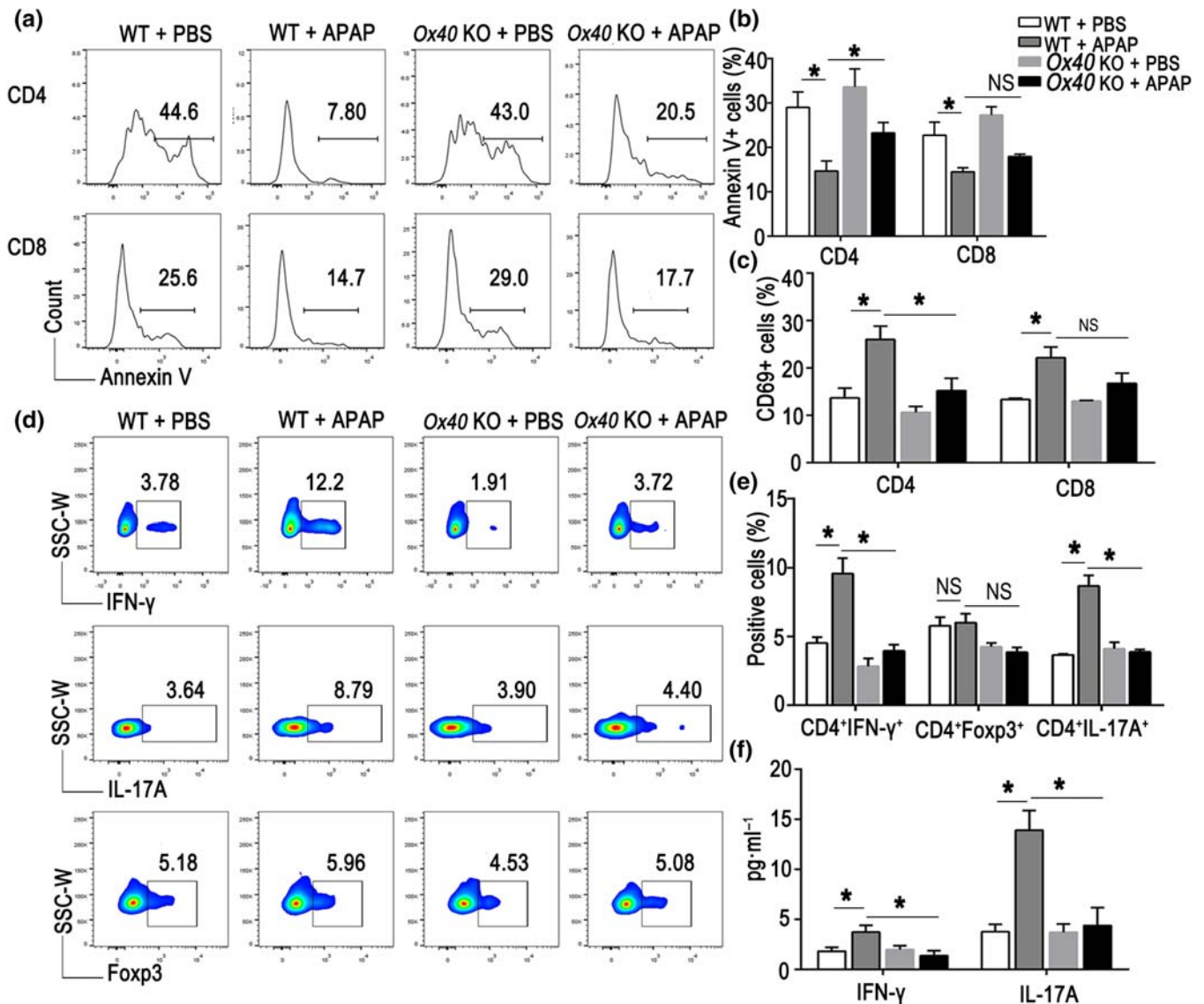


FIGURE 2 Ox40 KO reduces intrahepatic Th1 and Th17 cell differentiation in paracetamol (APAP)-induced liver injury. (a) Flow cytometry analysis of Annexin V⁺ cells relative to the total numbers of CD4⁺ and CD8⁺ T cells in liver tissue of mice from each group. (b) Statistical analysis of the percentages of Annexin V⁺ cells relative to the total number of intrahepatic CD4⁺ and CD8⁺ T cells. (c) Percentages of CD69⁺ cells relative to the total number of CD4⁺ and CD8⁺ T cells, determined by flow cytometry in the indicated groups. (d) Flow cytometry analysis of IFN-γ⁺ cells, Foxp3⁺ cells and IL-17A⁺ cells relative to the total number of CD4⁺ T cells in liver tissue in mice from each group. (e) Statistical analysis of the percentages of IFN-γ⁺ cells, Foxp3⁺ cells and IL-17A⁺ cells relative to the total number of intrahepatic CD4⁺ T cells, quantified by flow cytometry. (f) Plasma levels of IFN-γ and IL-17A, detected by flow cytometry. The data are presented as the mean ± SEM; control groups (n = 5) and treatment groups (n = 6). One-way ANOVA followed by Bonferroni's multiple comparison post hoc test was used for statistical analysis. *P < .05. NS, no significance

changed during acute liver injury (Figure 3d,g). In addition, the changes in plasma levels of TNF-α, IL-6, and IL-10 were similar to those observed in liver tissue during paracetamol-induced acute liver injury (Figure 3h).

We also examined the expression of M1 and M2 macrophage marker genes *iNOS* and *Arg-1*, respectively, in liver samples after paracetamol administration. As shown in Figure 3i, compared with the WT mice, *iNOS* mRNA levels were reduced, and *Arg-1* mRNA levels were increased in the liver of Ox40 KO mice, indicating that Ox40 affected macrophage M1/M2 polarization.

3.4 | OX40 on CD4⁺ T cells exacerbates paracetamol-induced acute liver injury and the pro-inflammatory state of intrahepatic macrophages

To further verify that OX40 on CD4⁺ T cells aggravates paracetamol-induced acute liver injury, we transferred CD4⁺ T cells from naïve WT or Ox40 KO mice to *Rag1*^{-/-} mice 16 hr before the paracetamol challenge (Figure 4a). Compared with the paracetamol-treated *Rag1*^{-/-} mice, adoptive transfer of CD4⁺ T cells resulted in significantly increased plasma alanine aminotransferase and aspartate

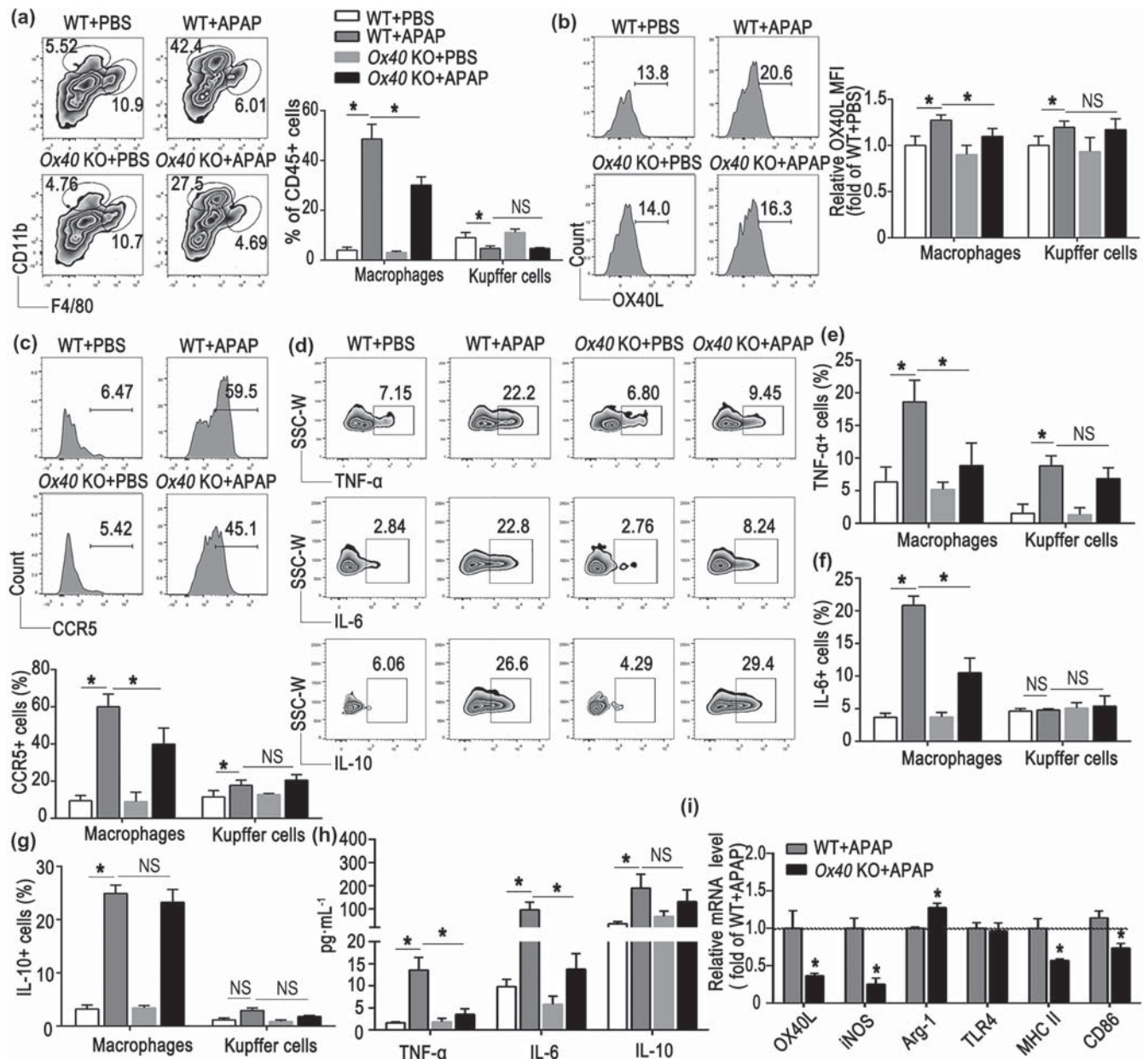


FIGURE 3 Ox40 KO alleviates liver injury by reducing the pro-inflammatory state of monocyte-derived macrophages. (a) Representative flow cytometry plots from liver CD45⁺ mononuclear cells (MNCs) showing populations of liver-infiltrating macrophages (CD11b^{int}F4/80^{low}) and Kupffer cells (CD11b^{low}F4/80^{hi}). Quantification of hepatic macrophages and Kupffer cells as a percentage of all liver CD45⁺ cells was shown. (b) Representative flow cytometry images of OX40L in hepatic macrophages and relative changes in OX40L expression were plotted as fold changes of those in WT + PBS group. (c) Representative flow cytometry images of CCR5 in hepatic macrophages and statistical analysis of the percentage CCR5. (d) Representative flow cytometry plots of TNF- α ⁺, IL-6⁺, and IL-10⁺ populations of hepatic macrophages. (e) Changes in the percentage of TNF- α ⁺ cells relative to the total number of macrophages and Kupffer cells in the liver. (f) Changes in the percentage of IL-6⁺ cells relative to the total number of macrophages and Kupffer cells in the liver. (g) Changes in the percentage of IL-10⁺ cells relative to the total number of macrophages and Kupffer cells in the liver. (h) Plasma levels of TNF- α , IL-6 and IL-10, determined by flow cytometry. (i) Quantitative real-time PCR analysis of OX40L, iNOS, Arg-1, TLR4, MHC II, and CD86 mRNA levels in the liver from each group. The data are presented as the mean \pm SEM; control groups ($n = 5$) and treatment groups ($n = 6$). Two-group comparisons were made by the unpaired Student's t -test, and multiple comparisons were analysed by one-way ANOVA followed by Bonferroni's post hoc test. * $P < .05$. NS, no significance

aminotransferase levels in the *Rag1*^{-/-} mice, which suggested that CD4⁺ T cells exacerbated paracetamol-induced acute liver injury. However, the *Rag1*^{-/-} mice that received CD4⁺ T cells from the Ox40 KO mice exhibited significantly lower plasma alanine aminotransferase

and aspartate aminotransferase levels (Figure 4b). Furthermore, histological analysis revealed reduced liver centrilobular necrosis in the *Rag1*^{-/-} mice upon an adoptive transfer of Ox40 KO-CD4⁺ T cells (Figure 4c).

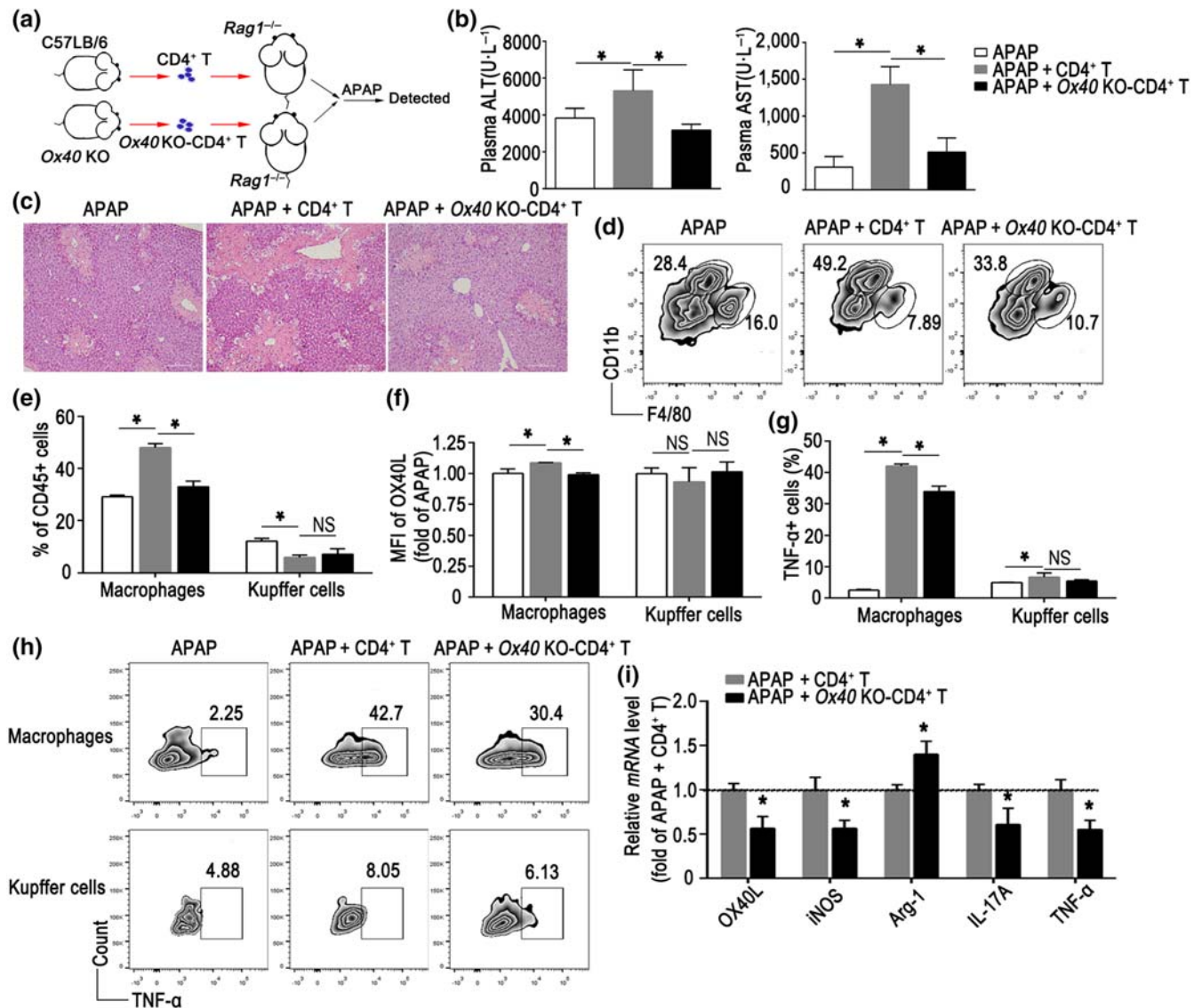


FIGURE 4 CD4⁺ T cells exacerbate paracetamol (APAP) induced acute liver injury (ALI) and regulate inflammation of intrahepatic macrophages via OX40. (a) Flow chart of adoptive transfer of WT or Ox40 KO-CD4⁺ T cells to Rag1^{-/-} mouse. (b) Plasma levels of alanine aminotransferase (ALT) and aspartate aminotransferase (AST). (c) H&E staining of the liver paraffin sections from each group. (d) Representative flow cytometry images showing the intrahepatic macrophage (CD11b^{int}F4/80^{low}) and Kupffer cell (CD11b^{low}F4/80^{hi}) populations. (e) Statistical analysis of the percentages of hepatic macrophages and Kupffer cells relative to the total number of hepatic CD45⁺ cells, determined by flow cytometry. (f) Relative changes in OX40L expression, plotted as fold changes of OX40L expression in mice from the APAP group. (g) Changes in the percentage of TNF-α⁺ cells relative to the total number of macrophages and Kupffer cells in the liver. (h) Flow cytometry plots of TNF-α⁺ cells arising from the hepatic macrophages and Kupffer cells. (i) Quantitative real-time PCR analysis of OX40L, iNOS, Arg-1, IL-17A and TNF-α mRNA levels in the liver. The data are presented as the mean ± SEM; n = 5 mice per group. Two-group comparisons were made by the unpaired Student's t-test, and multiple comparisons were analysed by one-way ANOVA followed by Bonferroni's post hoc test. *P < .05. NS, no significance

As shown in Figure 4d,e, the Rag1^{-/-} mice that harboured Ox40 KO-CD4⁺ T cells had a lower frequency of hepatic macrophages than the mice that received WT-CD4⁺ T cells. No difference was apparent in the percentage of Kupffer cells in the Rag1^{-/-} mice that received Ox40 KO-CD4⁺ T cells or WT-CD4⁺ T cells. Furthermore, the transfer of Ox40-deficient CD4⁺ T cells also down-regulated OX40L expression in macrophages, but not in Kupffer cells, compared with the transfer of WT-CD4⁺ T cells (Figure 4f).

Furthermore, the TNF-α production was dramatically increased in macrophages and Kupffer cells in the paracetamol-treated mice that

received WT-CD4⁺ T cells. The proportion of TNF-α-positive macrophages in paracetamol-treated mice that received Ox40 KO-CD4⁺ T cells was relatively lower (Figure 4g,h). No significant difference in the TNF-α secretion by Kupffer cells in the paracetamol-treated mice that received WT-CD4⁺ T cells or Ox40-CD4⁺ T cells was observed (Figure 4g,h). Consistent with the flow cytometry findings, the OX40L and TNF-α mRNA levels in the liver of the Rag1^{-/-} mice carrying Ox40-deficient CD4⁺ T cells were substantially reduced. Furthermore, 24 hr after the paracetamol treatment, the expression of iNOS mRNA was remarkably decreased in the liver of mice that harboured Ox40 KO-

CD4⁺ T cells, in contrast with the increasing trend of *Arg-1* mRNA expression in the liver. The *IL-17A* mRNA level was also reduced in the paracetamol-treated mice that received Ox40 KO-CD4⁺ T cells (Figure 4i).

3.5 | Soluble OX40 enhances pro-inflammatory cytokine secretion by hepatic macrophages and promotes liver injury

Considering the substantially increased plasma levels of soluble OX40 during paracetamol-induced acute liver injury, we proceeded to determine the role of soluble OX40 during paracetamol-induced acute liver injury. To identify the potential role of soluble OX40 in paracetamol-induced liver injury, *Rag1*^{-/-} mice were challenged with paracetamol. First, we compared the liver injury in the IgG- and OX40/Fc-treated groups administered 300 mg·kg⁻¹ paracetamol; no significant difference in the liver injury was apparent between the groups (Figure S4A,B). Considering the serious liver injury elicited by the 300 mg·kg⁻¹ paracetamol dose, we adopted a lower dose of

paracetamol (150 mg·kg⁻¹) in the ensuing experiments. *Rag1*^{-/-} mice were hence challenged with the low dose of paracetamol (150 mg·kg⁻¹), with or without the administration of soluble OX40/Fc. As shown in Figure 5a, the low-dose paracetamol injection did not result in elevated plasma alanine aminotransferase levels; however, OX40/Fc administration promoted liver injury in the *Rag1*^{-/-} mouse, with an increase in plasma alanine aminotransferase levels. Consequently, OX40/Fc injection increased the proportion of liver-infiltrating macrophages, although the change was not significant (Figure 5b). Furthermore, the OX40L and CCR5 expression was markedly increased on the liver-infiltrating macrophages in the *Rag1*^{-/-} mice that received OX40/Fc (Figure 5c,d). In addition, the TNF- α and IL-6 production was dramatically increased in hepatic macrophages, but not in Kupffer cells, after OX40/Fc injection (Figure 5e-g).

Further, we used RT-PCR to quantify the mRNA levels of genes associated with the biological functions of the macrophage in the liver. As shown in Figure 5h, compared with the IgG-administered mice, the hepatic levels of *OX40L* and *iNOS* mRNA were elevated in mice that received OX40/Fc. These observations indicated that

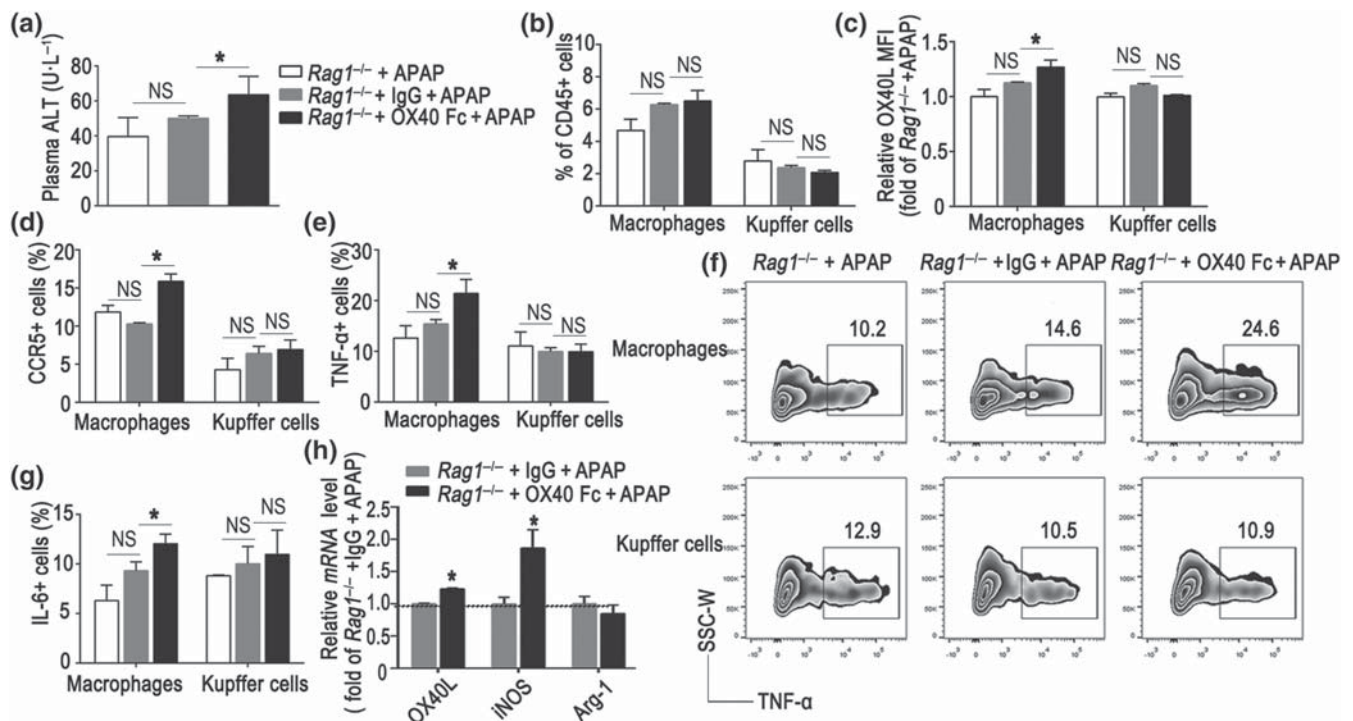


FIGURE 5 Soluble OX40 stimulation promotes liver injury and intrahepatic pro-inflammatory state. Soluble OX40 (OX40/Fc) was injected into *Rag1*^{-/-} mice challenged with 150 mg·kg⁻¹ paracetamol (APAP) and control mice administered isotype-matched IgG. (a) Plasma alanine aminotransferase (ALT) level. (b) Statistical analysis of the percentages of hepatic macrophages and Kupffer cells relative to the total number of hepatic CD45⁺ cells, measured by flow cytometry. (c) Relative changes in OX40L expression, plotted as fold changes of OX40L expression in *Rag1*^{-/-} mice from the APAP group. (d) Statistical analysis of CCR5 expression in hepatic macrophages and Kupffer cells, measured by flow cytometry. (e) Changes in the percentage of TNF- α ⁺ cells relative to the total number of macrophages and Kupffer cells in the liver. (f) Representative flow cytometry plots of TNF- α ⁺ cells arising from the hepatic macrophages and Kupffer cells. (g) Changes in the percentage of IL-6⁺ cells relative to the total number of macrophages and Kupffer cells in the liver. (h) Quantitative real-time PCR analysis of *OX40L*, *iNOS*, and *Arg-1* mRNA levels in the liver. The data are presented as the mean \pm SEM; $n = 5$ mice per group. Two-group comparisons were made by the unpaired Student's t test, and multiple comparisons were analysed by one-way ANOVA followed by Bonferroni's post hoc test. * $P < .05$. NS, no significance

soluble OX40 promoted hepatic macrophage polarization towards the M1 pro-inflammatory phenotype.

3.6 | OX40 stimulation enhances the pro-inflammatory state of murine macrophage

To determine whether macrophages were affected directly by OX40, we stimulated the murine macrophage cell lines RAW264.7 and J774A.1 with different concentrations of soluble OX40/Fc for 2 days. As shown in Figure S4C,D, all concentrations of OX40/Fc tested (especially $2.0 \mu\text{g}\cdot\text{ml}^{-1}$) up-regulated the production of functional molecules by macrophages. We therefore used the $2.0 \mu\text{g}\cdot\text{ml}^{-1}$ dose of OX40/Fc in the ensuing experiments. As shown in Figure 6a, OX40/Fc stimulation significantly up-regulated the expression of chemokine receptors (CCR2, CCR5, CCR7, CCR9, CXCR3 and CXCR5) and antigen processing and presenting molecules (TLR4, OX40L, MHC II, CD40 and CD86) in the RAW64.7 cells compared with the IgG-treated cells. The same trend was apparent in OX40/Fc-treated J774A.1 cells (Figure 6b). Furthermore, when the OX40/OX40L signalling pathway was blocked with an OX40L neutralizing antibody, the up regulation of these molecules was diminished in both RAW264.7 and J774A.1 cells. As shown in Figure 6a,b, OX40/Fc treatment significantly increased the secretion of these pro-inflammatory cytokines.

Hypoxia-inducible factor 1 α (Hif1 α) is a key nucleoprotein with a transcriptional activity that up-regulates the expression of pro-inflammatory cytokine genes in macrophage (Corcoran & O'Neill, 2016). As shown in Figure 6c–e, OX40/Fc treatment substantially increased the hypoxia-inducible factor 1 alpha expression in RAW264.7 and J774A.1 cells, as determined by both flow cytometry and RT-PCR. These observations indicated that OX40/Fc might up-regulate macrophage pro-inflammatory state by promoting hypoxia-inducible factor 1 alpha overexpression.

3.7 | OX40 levels are elevated in drug-induced liver injury in human

To determine whether the above findings are relevant for human, we next analysed the plasma OX40 levels in 26 drug-induced liver injury patients and 31 healthy controls. The demographic and clinical characteristics of the individuals were shown in Table S2. Notably, the OX40 plasma levels in drug-induced liver injury patients were higher when compared to those of the healthy controls (Figure 6f). Elevated serum levels of alanine aminotransferase, aspartate aminotransferase, total bilirubin (TBIL), direct bilirubin (DBIL) and albumin (ALB) are important markers for assessing the severity of liver injury. Positive correlation was observed between the plasma OX40 and serum alanine aminotransferase and aspartate aminotransferase levels. In addition, we noted positive correlation between the plasma OX40 and serum total bilirubin and direct bilirubin levels. However, no correlation was apparent between the plasma OX40 levels and albumin levels

(Figure 6g). These observations suggested that OX40 is involved in drug-induced liver injury development in human.

4 | DISCUSSION

Intrahepatic immune cells are activated by necrotic hepatocytes during paracetamol overdose and the ensuing immune responses play critical roles in the development of liver injury (Szabo & Petrasek, 2015). During acute liver failure, the levels of adhesion molecules and chemokines are locally increased within the hepatic parenchyma and contribute to the recruitment of lymphocytes to the liver (Tuncer, Oo, Murphy, Adams, & Lalor, 2013). In the current study we revealed that OX40, which belongs to the TNF superfamily of proteins and is generally identified on activated memory T lymphocytes (Webb, Hirschfeld, & Lane, 2016), was predominantly overexpressed on liver-infiltrating CD4⁺ T cells during liver injury. Increased OX40 levels on CD4⁺ T cells could bind OX40L on antigen-presenting cells in the injured liver. Further, OX40 stimulation selectively promoted Th1 and Th17 differentiation and reduced CD4⁺ T-cell apoptosis, thus exacerbating liver injury. This indicated that the OX40 molecule on CD4⁺ T cells plays a critical role in paracetamol-induced liver injury.

To date, studies of the OX40–OX40L interaction have mainly focused on the regulation of conventional T cells. According to several studies, OX40 can also regulate other immune cells, in addition to T cells, for example enhancing CD40L signals of B cells, promoting endothelial cell trans-endothelial migration and increasing dendritic cell maturation with CD83 expression (Jourdan et al., 2000; Ohshima et al., 1997; Stuber & Strober, 1996). However, the potential mechanisms that underlie these phenomena are unknown.

To explore whether OX40 on CD4⁺ T cells affects the macrophage response in paracetamol-induced liver injury, we transferred WT-CD4⁺ T and *Ox40* KO-CD4⁺ T cells to *Rag1*^{-/-} mice and then induced acute liver injury by a paracetamol overdose. We observed that *Ox40* KO-CD4⁺ T cells alleviated the liver injury, not only affecting the migration of macrophages to the injury sites via OX40/OX40L, but also antigen presentation and inflammatory cytokine secretion by macrophages. This suggested that OX40 serves as a bridge, regulating the interaction between innate immune cells and adaptive immune cells.

The role of liver-infiltrating macrophages in liver injury is controversial. Dambach, Watson, Gray, Durham, and Laskin (2002) reported that at a relatively late stage of paracetamol-induced liver injury, the infiltrating macrophages repair the damaged liver tissue. According to another study, the infiltrating CCR2⁺ monocytes aggravate the early phase of paracetamol-induced acute liver injury (Mossanen et al., 2016). In addition, a recent report points that the macrophages infiltrating an injury tissue tend to be pro-inflammatory, with the tissue-resident macrophages playing a protective role (Hoyer et al., 2019). In the current study, we detected recruited macrophages at an early phase after the paracetamol challenge and observed that *Ox40* knock-out reduced the production of TNF- α and IL-6 pro-inflammatory cytokines by macrophages.

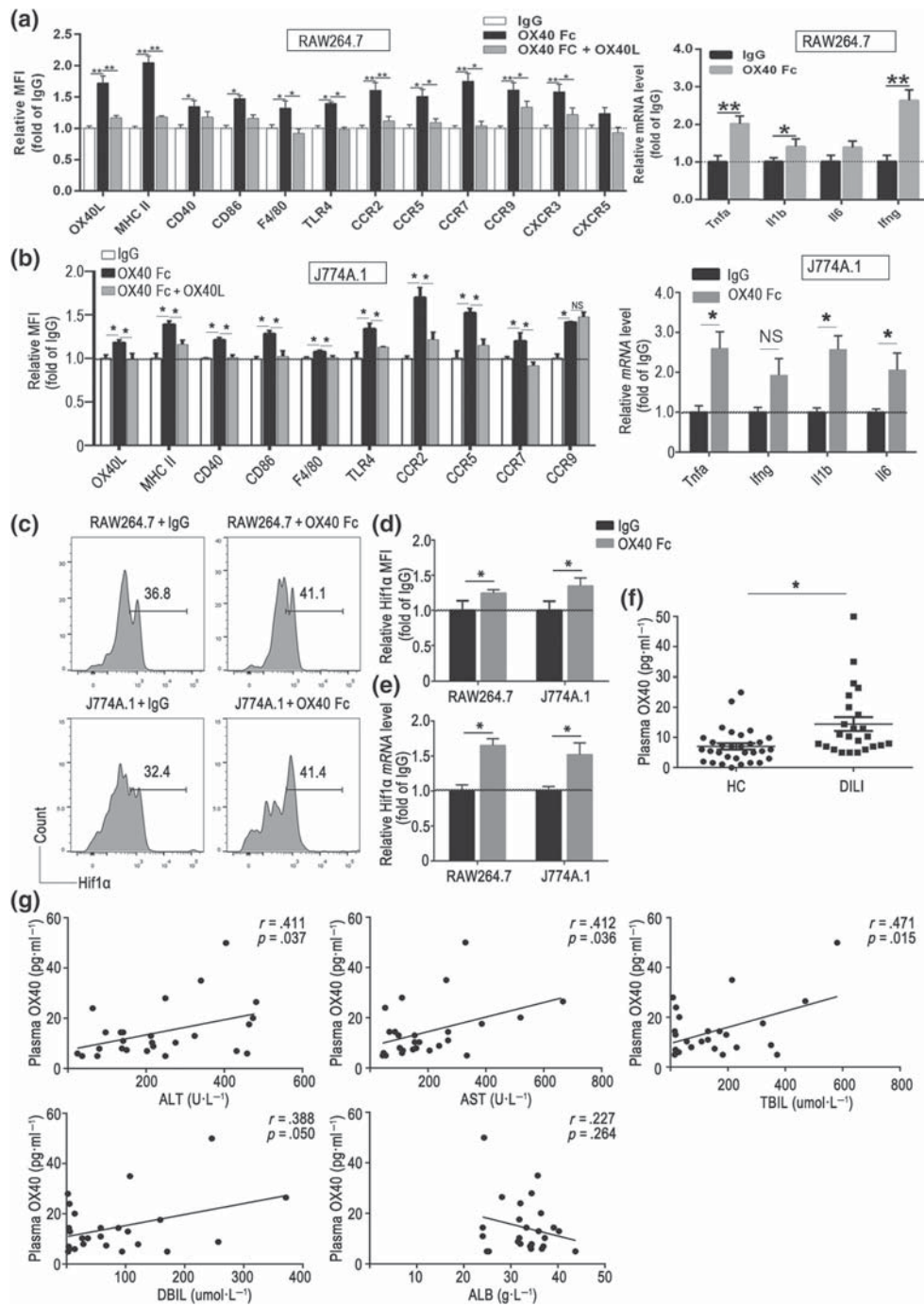


FIGURE 6 Soluble OX40 stimulation enhances the pro-inflammatory state of murine macrophage. (a) Expression of antigen presentation-associated molecules and chemokine receptors in RAW264.7 cells, determined by flow cytometry, and quantitative real-time PCR analysis of the pro-inflammatory cytokine mRNA levels in OX40/Fc-stimulated RAW264.7 cells. (b) Expression of antigen presentation-associated molecules and chemokine receptors in J774A.1 cells, determined by flow cytometry, and quantitative real-time PCR analysis of the pro-inflammatory cytokine mRNA levels in OX40/Fc-stimulated J774A.1 cells. (c) Representative flow cytometry images of hypoxia-inducible factor 1 alpha ($Hif1\alpha$) population among OX40/Fc-stimulated RAW264.7 and J774A.1 cells. (d) Relative changes in $Hif1\alpha$ expression, plotted as fold changes of $Hif1\alpha$ expressed in the IgG-treated group. (e) Quantitative real-time PCR analysis of $Hif1\alpha$ mRNA level in OX40/Fc-stimulated RAW264.7 and J774A.1 cells. (f) Plasma soluble OX40 levels determined by ELISA in HC and drug-induced liver injury (DILI) patients. (g) Evidence of significant positive correlation between the plasma OX40 and serum alanine aminotransferase (ALT), aspartate aminotransferase (AST), total bilirubin (TBIL) and direct bilirubin (DBIL) levels and lack of significant correlation between the plasma OX40 and albumin (ALB) levels ($n = 26$). The data are presented as the mean \pm SEM. Two-group comparisons were made by the unpaired Student's t -test, and multiple comparisons were analysed by one-way ANOVA followed by Bonferroni's post hoc test. While for the clinical study data, normal variable distributions were tested using the Shapiro–Wilk test. Spearman's correlation coefficient was used to estimate the association of plasma OX40 levels and ALT, AST, TBIL, DBIL and ALB. * $P < .05$. NS, no significance

In the current study, we also observed a significant increase in soluble plasma OX40 levels and enhanced liver infiltration of M1 macrophages in paracetamol-induced liver injury. Although the pro-inflammatory cytokines IFN- γ and IL-17 produced by Th1 and Th17 cells can affect the M1 polarization of macrophages, we speculated that OX40 might be involved in the regulation of innate immune cells in addition to the effect on cytokine secretion. The *in vivo* and *in vitro* treatment with soluble OX40/Fc indicated that OX40 alone could regulate antigen presentation and pro-inflammatory cytokine secretion by macrophages and that increased macrophage hypoxia-inducible factor 1 alpha expression was involved in these effects.

There are several limitations in this study. First, we showed that soluble OX40 regulated antigen presentation and pro-inflammatory cytokine secretion by macrophages, and we also provided evidence that OX40 up-regulated murine macrophage pro-inflammatory state by increasing hypoxia-inducible factor 1 alpha expression. However, the signalling pathways linking OX40L engagement with the observed inflammatory consequences in macrophage must be explored further. Second, we observed that individuals with drug-induced liver injury exhibited significantly higher OX40 plasma levels than healthy controls. This indicates that OX40 may be an important regulator and a potential contributor to human drug-induced liver injury development and progression. However, long-term follow-up of the levels of OX40 in the same subjects in the progressive and remission stages of drug-induced liver injury should be performed, to allow further assessment of the importance of OX40 in the pathology of drug-induced liver injury.

In summary, we observed that OX40 levels were significantly elevated in drug-induced liver injury patients. During paracetamol-induced liver injury, OX40 expression was increased predominantly on CD4⁺ T cells. Further, OX40 promoted intrahepatic CD4⁺ T-cell activation, and differentiation into Th1 and Th17 cells. Furthermore, OX40L expression was up-regulated in infiltrating macrophages during liver injury. The OX40–OX40L interaction increased the hypoxia-inducible factor 1 alpha expression and enhanced antigen presentation, migration, and pro-inflammatory cytokine secretion by liver-infiltrating macrophages. The OX40-enhanced innate and adaptive immunity ultimately exacerbated the paracetamol-induced liver injury. Collectively, OX40 is a key molecule that mediates both intrahepatic innate and adaptive immunity and promotes both pro-inflammatory macrophage and CD4⁺ T-cell function, thus exacerbating drug-induced liver injury. OX40 may thus serve as a diagnostic index and therapeutic target of drug-induced liver injury.

ACKNOWLEDGEMENTS

This study was supported by grants from the National Natural Science Foundation of China (81870399, 81900526, and 81970503).

AUTHOR CONTRIBUTIONS

All listed authors participated meaningfully in the study and that they have seen and approved the submission of this manuscript. C.Z., H.J., and Y.W. participated in performing the research, analysing the data, and initiating the original draft of the article. C.L., X.Z., Y.L., W.S., Y.T.,

H.X., D.T., and K.L. participated in performing the research and collecting the data. D.Z., J.J., and G.S. established the hypotheses, supervised the studies, analysed the data, and co-wrote the manuscript.

CONFLICT OF INTEREST

All authors have no conflicts of interest to declare.

DECLARATION OF TRANSPARENCY AND SCIENTIFIC RIGOUR

This Declaration acknowledges that this paper adheres to the principles for transparent reporting and scientific rigour of preclinical research as stated in the BJP guidelines for Design & Analysis, Immunoblotting and Immunochemistry, and Animal Experimentation, and as recommended by funding agencies, publishers and other organisations engaged with supporting research.

ORCID

Dong Zhang  <https://orcid.org/0000-0002-3404-5173>

REFERENCES

- Alexander, S. P. H., Fabbro, D., Kelly, E., Mathie, A., Peters, J. A., Veale, E. L., ... CGTP Collaborators. (2019a). The concise guide to pharmacology 2019/20: Catalytic receptors. *British Journal of Pharmacology*, 176(Suppl 1), S247–S296.
- Alexander, S. P. H., Fabbro, D., Kelly, E., Mathie, A., Peters, J. A., Veale, E. L., ... CGTP Collaborators. (2019b). The concise guide to pharmacology 2019/20: Enzymes. *British Journal of Pharmacology*, 176 (Suppl 1), S297–S396.
- Alexander, S. P. H., Roberts, R. E., Broughton, B. R. S., Sobey, C. G., George, C. H., Stanford, S. C., ... Ahluwalia, A. (2018). Goals and practicalities of immunoblotting and immunohistochemistry: A guide for submission to the British Journal of Pharmacology. *British Journal of Pharmacology*, 175, 407–411. <https://doi.org/10.1111/bph.14112>
- Andrade, R. J., Chalasani, N., Bjornsson, E. S., Suzuki, A., Kullak-Ublick, G. A., Watkins, P. B., ... Aithal, G. P. (2019). Drug-induced liver injury. *Nature Reviews. Disease Primers*, 5, 58. <https://doi.org/10.1038/s41572-019-0105-0>
- Cavaliere, M. L., & D'Agostino, D. (2017). Drug-, herb- and dietary supplement-induced liver injury. *Archivos Argentinos de Pediatría*, 115, e397–e403. <https://doi.org/10.5546/aap.2017.eng.e397>
- Corcoran, S. E., & O'Neill, L. A. (2016). HIF1alpha and metabolic reprogramming in inflammation. *The Journal of Clinical Investigation*, 126, 3699–3707.
- Croft, M., So, T., Duan, W., & Soroosh, P. (2009). The significance of OX40 and OX40L to T-cell biology and immune disease. *Immunological Reviews*, 229, 173–191. <https://doi.org/10.1111/j.1600-065X.2009.00766.x>
- Curtis, M. J., Alexander, S., Cirino, G., Docherty, J. R., George, C. H., Gienbycz, M. A., ... Ahluwalia, A. (2018). Experimental design and analysis and their reporting II: Updated and simplified guidance for authors and peer reviewers. *British Journal of Pharmacology*, 175, 987–993. <https://doi.org/10.1111/bph.14153>
- Dambach, D. M., Watson, L. M., Gray, K. R., Durham, S. K., & Laskin, D. L. (2002). Role of CCR2 in macrophage migration into the liver during acetaminophen-induced hepatotoxicity in the mouse. *Hepatology*, 35, 1093–1103.
- European Association for the Study of the Liver. Electronic address: easloffice@easloffice.eu, Clinical Practice Guideline Panel: Chair, Panel members, & EASL Governing Board representative. (2019). EASL Clinical Practice Guidelines: Drug-induced liver injury. *Journal of*

- Hepatology*, 70, 1222–1261. <https://doi.org/10.1016/j.jhep.2019.02.014>
- Harding, S. D., Sharman, J. L., Faccenda, E., Southan, C., Pawson, A. J., Ireland, S., ... NC-IUPHAR. (2018). The IUPHAR/BPS guide to pharmacology in 2018: Updates and expansion to encompass the new guide to IMMUNOPHARMACOLOGY. *Nucleic Acids Research*, 46, D1091–D1106. <https://doi.org/10.1093/nar/gkx1121>
- Hoyer, F. F., Naxerova, K., Schloss, M. J., Hulsmans, M., Nair, A. V., Dutta, P., ... Nahrenndorf, M. (2019). Tissue-specific macrophage responses to remote injury impact the outcome of subsequent local immune challenge. *Immunity*, 51, 899–914 e897.
- Jaeschke, H., Williams, C. D., Ramachandran, A., & Bajt, M. L. (2012). Acetaminophen hepatotoxicity and repair: The role of sterile inflammation and innate immunity. *Liver International*, 32, 8–20. <https://doi.org/10.1111/j.1478-3231.2011.02501.x>
- Jourdan, P., Vendrell, J. P., Huguet, M. F., Segondy, M., Bousquet, J., Pene, J., & Yssel, H. (2000). Cytokines and cell surface molecules independently induce CXCR4 expression on CD4⁺ CCR7⁺ human memory T cells. *Journal of Immunology*, 165, 716–724. <https://doi.org/10.4049/jimmunol.165.2.716>
- Kilkenny, C., Browne, W., Cuthill, I. C., Emerson, M., & Altman, D. G. (2010). Animal research: Reporting *in vivo* experiments: the ARRIVE guidelines. *British Journal of Pharmacology*, 160, 1577–1579.
- Kim, S. J., Kim, K. M., Yang, J. H., Cho, S. S., Kim, J. Y., Park, S. J., ... Ki, S. H. (2017). Sestrin2 protects against acetaminophen-induced liver injury. *Chemico-Biological Interactions*, 269, 50–58. <https://doi.org/10.1016/j.cbi.2017.02.002>
- Krenkel, O., Mossanen, J. C., & Tacke, F. (2014). Immune mechanisms in acetaminophen-induced acute liver failure. *Hepatobiliary Surgery and Nutrition*, 3, 331–343.
- McGrath, J. C., Drummond, G. B., McLachlan, E. M., Kilkenny, C., & Wainwright, C. L. (2010). Guidelines for reporting experiments involving animals: The ARRIVE guidelines. *British Journal of Pharmacology*, 160, 1573–1576. <https://doi.org/10.1111/j.1476-5381.2010.00873.x>
- McGrath, J. C., & Lilley, E. (2015). Implementing guidelines on reporting research using animals (ARRIVE etc.): New requirements for publication in BJP. *British Journal of Pharmacology*, 172, 3189–3193. <https://doi.org/10.1111/bph.12955>
- Mederacke, I., Dapito, D. H., Affo, S., Uchinami, H., & Schwabe, R. F. (2015). High-yield and high-purity isolation of hepatic stellate cells from normal and fibrotic mouse livers. *Nature Protocols*, 10, 305–315. <https://doi.org/10.1038/nprot.2015.017>
- Mossanen, J. C., Krenkel, O., Ergen, C., Govaere, O., Liepelt, A., Puengel, T., ... Tacke, F. (2016). Chemokine (C-C motif) receptor 2-positive monocytes aggravate the early phase of acetaminophen-induced acute liver injury. *Hepatology*, 64, 1667–1682. <https://doi.org/10.1002/hep.28682>
- Mossanen, J. C., & Tacke, F. (2015). Acetaminophen-induced acute liver injury in mice. *Laboratory Animals*, 49, 30–36. <https://doi.org/10.1177/0023677215570992>
- Numata, K., Kubo, M., Watanabe, H., Takagi, K., Mizuta, H., Okada, S., ... Matsukawa, A. (2007). Overexpression of suppressor of cytokine signaling-3 in T cells exacerbates acetaminophen-induced hepatotoxicity. *Journal of Immunology*, 178, 3777–3785. <https://doi.org/10.4049/jimmunol.178.6.3777>
- Ohshima, Y., Tanaka, Y., Tozawa, H., Takahashi, Y., Maliszewski, C., & Delespesse, G. (1997). Expression and function of OX40 ligand on human dendritic cells. *Journal of Immunology*, 159, 3838–3848.
- Stuber, E., & Strober, W. (1996). The T cell-B cell interaction via OX40-OX40L is necessary for the T cell-dependent humoral immune response. *The Journal of Experimental Medicine*, 183, 979–989. <https://doi.org/10.1084/jem.183.3.979>
- Szabo, G., & Petrasek, J. (2015). Inflammasome activation and function in liver disease. *Nature Reviews. Gastroenterology & Hepatology*, 12, 387–400.
- Tuncer, C., Oo, Y. H., Murphy, N., Adams, D. H., & Lalor, P. F. (2013). The regulation of T-cell recruitment to the human liver during acute liver failure. *Liver International*, 33, 852–863. <https://doi.org/10.1111/liv.12182>
- Wang, X., Sun, R., Chen, Y., Lian, Z. X., Wei, H., & Tian, Z. (2015). Regulatory T cells ameliorate acetaminophen-induced immune-mediated liver injury. *International Immunopharmacology*, 25, 293–301.
- Ward-Kavanagh, L. K., Lin, W. W., Sedy, J. R., & Ware, C. F. (2016). The TNF receptor superfamily in co-stimulating and co-inhibitory responses. *Immunity*, 44, 1005–1019.
- Webb, G. J., Hirschfield, G. M., & Lane, P. J. (2016). OX40, OX40L and Autoimmunity: A comprehensive review. *Clinical Reviews in Allergy and Immunology*, 50, 312–332. <https://doi.org/10.1007/s12016-015-8498-3>
- Zhao, H. J., Li, M. J., Zhang, M. P., Wei, M. K., Shen, L. P., Jiang, M., & Zeng, T. (2019). Allyl methyl trisulfide protected against acetaminophen (paracetamol)-induced hepatotoxicity by suppressing CYP2E1 and activating Nrf2 in mouse liver. *Food & Function*, 10, 2244–2253. <https://doi.org/10.1039/C9FO00170K>
- Zhu, X., & Uetrecht, J. (2013). A novel T_H17-type cell is rapidly increased in the liver in response to acetaminophen-induced liver injury: T_H17 cells and the innate immune response. *Journal of Immunotoxicology*, 10, 287–291.

SUPPORTING INFORMATION

Additional supporting information may be found online in the Supporting Information section at the end of this article.

How to cite this article: Zhang C, Jin H, Wang Y, et al. Critical role of OX40 in drug-induced acute liver injury. *Br J Pharmacol*. 2020;177:3183–3196. <https://doi.org/10.1111/bph.15041>